

# QCD at High Parton Density

V. P. Gonçalves

*Instituto de Física e Matemática, Universidade Federal de Pelotas*

*Caixa Postal 354, CEP 96010-090, Pelotas, RS, Brazil*

Received on 11 December, 2003

The high parton density regime of Quantum Chromodynamics (QCD) is briefly discussed. Some phenomenological aspects of saturation are described, mainly focusing on possible signatures of the non-linear QCD dynamics in electron-proton/nucleus collisions. Implications of these effects in central and ultraperipheral heavy-ion collisions are also presented.

## 1 Introduction

The high parton density regime in deep inelastic electron-proton (nucleus) scattering is characterized by small values of the Bjorken variable  $x = Q^2/s$ , where  $Q^2$  is the momentum transfer and  $\sqrt{s}$  is the center of mass energy, and represents the challenge of studying the interface between the perturbative and nonperturbative QCD, with the peculiar feature that this transition is taken in a kinematical region where the strong coupling constant  $\alpha_s$  is small. By the domain of perturbative QCD we mean the region where the parton picture has been developed and the separation between the short and long distance contributions (the collinear factorization) is made possible by the use of the operator product expansion (OPE). The Dokshitzer-Gribov-Lipatov-Altarelli-Parisi (DGLAP) equations [1] are the evolution equations in this kinematical region. In the limit of small values of  $x$  ( $< 10^{-2}$ ) one expects to see new features inside the nucleon: the density of gluons and quarks become very high and an associated new dynamical effect is expected to stop the further growth of the structure functions. In particular, for a fixed hard scale  $Q^2 \gg \Lambda_{QCD}^2$ , the OPE eventually breaks down at sufficiently small  $x$  [2]. Ultimately, the physics in the region of high parton densities will be described by nonperturbative methods, which is still waiting for a satisfactory solution in QCD. However, the transition from the moderate  $x$  region towards the small  $x$  limit may possibly be accessible in perturbation theory, and, hence, allows us to test the ideas about the onset of nonperturbative dynamics.

The expectation of the transition for the high density regime can be understood considering the physical picture of the deep inelastic scattering. In the infinite momentum frame (IMF) the virtual photon with virtuality  $Q^2$  measures the number density of charged partons having longitudinal momentum fraction  $x$  and transverse spatial size  $\Delta x_\perp \leq 1/Q$ . When  $Q^2$  is large,  $\alpha_s(Q^2)$  is small, so that the struck quark can be treated perturbatively. Also, when  $Q^2$  is large the struck quark is small, so that one can picture the struck quark as being isolated, far away from similar quarks,

in the proton. Thus, so long as the parton distributions are not large, the partons in a proton are dilute. However, if the parton distributions get large enough, which happens when  $x$  is very small, partons in the proton must begin to overlap. If there is a sufficient amount of parton overlap then a given parton will not act as a free quantum over its lifetime but will interact strongly with the other partons in the proton, even though  $\alpha_s$  may still be in the perturbative regime. In other words, while for large momentum transfer  $k_\perp$ , the linear evolution equations (DGLAP/BFKL) predicts that the mechanism  $g \rightarrow gg$  populates the transverse space with a large number of small size gluons per unit of rapidity (the transverse size of a gluon with momentum  $k_\perp$  is proportional to  $1/k_\perp$ ), for small  $k_\perp$  the produced gluons overlap and fusion processes,  $gg \rightarrow g$ , are equally important. Considering the latter process, the rise of the gluon distribution below a typical scale is reduced, restoring the unitarity. That typical scale is energy dependent and is called saturation scale  $Q_s$ . The saturation momentum sets the critical transverse size for the unitarization of the cross sections. Therefore, at sufficient small values of  $x$ , one enters in the regime of high density QCD, where partons from neighboring ladders overlap spatially and new dynamical effects associated with the unitarity corrections are expected to stop further growth of the parton densities.

Other important aspect which must be considered for the description of the QCD at high energies is that the usual collinear factorization approach for the calculations of the observables has to be replaced by a corresponding high energy ( $k_\perp$ -dependent) factorization in this regime. In the collinear factorization approach [3] all partons involved are assumed to be on mass shell, carrying only longitudinal momenta, and their transverse momenta are neglected in the QCD matrix elements. Moreover, the cross sections for the QCD subprocess are usually calculated in the leading order (LO), as well as in the next-to-leading order (NLO). In particular, the cross sections involving incoming hadrons are given, at all orders, by the convolution of intrinsically non-perturbative (but universal) quantities - the parton densities - with perturbatively calculable hard matrix elements, which are process

dependent. The conventional gluon distribution  $g(x, \mu^2)$ , which drives the behavior of the observables at high energies, corresponds to the density of gluons in the proton having a longitudinal momentum fraction  $x$  at the factorization scale  $\mu$ . This distribution satisfies the DGLAP evolution in  $\mu^2$  and does not contain information about the transverse momenta  $k_\perp$  of the gluon. On the other hand, in the large energy (small- $x$ ) limit, we have that the characteristic scale  $\mu$  of the hard subprocess of parton scattering is much less than  $\sqrt{s}$ , but greater than the  $\Lambda_{QCD}$  parameter. In this limit, the effects of the finite transverse momenta of the incoming partons become important, and the factorization must be generalized, implying that the cross sections are now  $k_\perp$ -factorized into an off-shell partonic cross section and a  $k_\perp$ -unintegrated parton density function  $\mathcal{F}(x, k_\perp)$ , characterizing the  $k_\perp$ -factorization approach [4]. The function  $\mathcal{F}$  is obtained as a solution of the evolution equation associated to the dynamics that governs the QCD at high energies.

The understanding and analytic description of the QCD at high energies has become an increasingly active subject of research, both from experimental and theoretical points of view. Theoretically, we expect that the growth of parton distributions should saturate, possibly forming a color glass condensate (CGC) [5], which is characterized by a bulk momentum scale  $Q_s$ . If the saturation scale is larger than the QCD scale  $\Lambda_{QCD}$ , then this regime can be studied using weak coupling methods. The magnitude of  $Q_s$  is associated to the behavior of the gluon distribution at high energies, and some estimates have been obtained. In general, the predictions are  $Q_s \sim 1 \text{ GeV}$  at HERA/RHIC and  $Q_s \sim 2 - 3 \text{ GeV}$  at LHC [6, 7, 8]. In particular, it has been observed that the  $ep$  deep inelastic scattering (DIS) data at low  $x$  can be successfully described with the help of the saturation model [6], which incorporates the main characteristics of the high density QCD approaches [9, 10, 5]. On the other hand, deep inelastic scattering on nuclei gives us a new possibility to reach high-density QCD phase without requiring extremely low values of  $x$ . The nucleus in this process serves as an amplifier for nonlinear phenomena expected in QCD at small  $x$ . In order to understand this expectation and estimate the kinematic region where the high densities effects should be present, we can analyze the behavior of the function  $\kappa(x, Q^2) \equiv \frac{3\pi^2 \alpha_s}{2Q^2} \frac{x g_A(x, Q^2)}{\pi R_A^2}$ , which represents the probability of gluon-gluon interaction inside the parton cascade, and also is denoted the packing factor of partons in a parton cascade [11, 10]. Considering that the condition  $\kappa = 1$  specifies the critical line, which separates between the linear (low parton density) regime  $\kappa \ll 1$  and the high density regime  $\kappa \gg 1$ , we can define the saturation momentum scale  $Q_s$  given by

$$Q_s^2(x; A) = \frac{3\pi^2 \alpha_s}{2} \frac{x g_A(x, Q_s^2(x; A))}{\pi R_A^2} , \quad (1)$$

below which the gluon density reaches its maximum value (saturates). At any value of  $x$  there is a value of  $Q^2 = Q_s^2(x)$  in which the gluonic density reaches a sufficiently high value that the number of partons stops to rise. This scale depends on the energy of the process [ $x g \propto x^{-\lambda}$  ( $\lambda \approx 0.3$ )] and on the atomic number of the colliding nuclei [ $R_A \propto A^{1/3} \rightarrow$

$Q_s^2 \propto A^{1/3}$ ], with the saturation scale for nuclear targets larger than for nucleon ones [Fig. 1]. This result motivates more extensive studies of nuclear collisions and, in particular, of electron-nucleus collisions at high energies, where the number of other medium effects is reduced in comparison with  $AA$  collisions.

In that follows we present a brief review of some signatures of the high parton density regime (For other recent reviews see Refs. [12, 13, 14]). In the next section, we discuss the high density effects in the deep inelastic scattering process and the property of geometric scaling predicted theoretically and observed in the HERA data. Moreover, some signatures of these effects in electron-nuclei collisions are proposed. In Section 3 the possibility of using ultraperipheral heavy ion collisions as a photonuclear collider is analyzed and some predictions for the saturation effects in the heavy quark production are presented. In Section 4 we discuss the saturation effects in nuclear collisions. In particular, we present some estimates for these effects in the signatures of the quark-gluon plasma. Finally, in Section 5 we summarize our main conclusions.

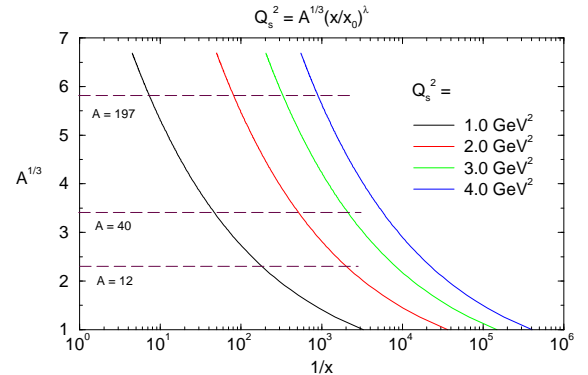


Figure 1. Saturation scale for different values of  $A$  and  $x$ .

## 2 Seeking Saturation in $ep/eA$ Processes

We start from the space-time picture of the  $ep$  processes [15]. The deep inelastic scattering  $ep \rightarrow e + X$  is characterized by a large electron energy loss  $\nu$  (in the target rest frame) and an invariant momentum transfer  $q^2 \equiv -Q^2$  between the incoming and outgoing electron such that  $x = Q^2/2m_N\nu$  is fixed. In terms of Fock states we then view the  $ep$  scattering as follows: the electron emits a photon ( $|e\rangle \rightarrow |e\gamma\rangle$ ) with  $E_\gamma = \nu$  and  $p_{t\gamma}^2 \approx Q^2$ , after the photon splits into a  $q\bar{q}$  ( $|e\gamma\rangle \rightarrow |eq\bar{q}\rangle$ ) and typically travels a distance  $l_c \approx 1/m_N x$ , referred as the coherence length, before interacting in the nucleon. For small  $x$  (large  $s$ , where  $\sqrt{s}$  is the  $\gamma^* p$  center-of-mass energy), the photon converts to a quark pair at a large distance before it interacts to the target. Consequently, the space-time picture of the DIS in the target rest frame can be viewed as the decay of the virtual photon at high energy (small  $x$ ) into a quark-antiquark pair

long before the interaction with the target. The  $q\bar{q}$  pair subsequently interacts with the target. In the small  $x$  region, where  $x \ll \frac{1}{2mR}$ , the  $q\bar{q}$  pair crosses the target with fixed transverse distance  $r_\perp$  between the quarks. Following Gribov [16], we may write a double dispersion relation for the forward  $\gamma^* p$  elastic amplitude  $\mathcal{A}$ , related to the total cross section by the optical theorem ( $\text{Im } \mathcal{A} = s\sigma^{\gamma^* p}(s, Q^2)$ ), and obtain for fixed  $s$

$$\sigma^{\gamma^* p}(s, Q^2) = \sum_q \int \frac{dM^2}{M^2 + Q^2} \frac{dM'^2}{M'^2 + Q^2} \rho(s, M^2, M'^2) \times \frac{1}{s} \text{Im } \mathcal{A}_{q\bar{q}+p}(s, M^2, M'^2), \quad (2)$$

where  $M$  and  $M'$  are the invariant masses of the incoming and outgoing  $q\bar{q}$  pair. If we assume that the forward  $q\bar{q} + p$  scattering does not change the momentum of the quarks then  $\mathcal{A}_{q\bar{q}+p}$  is proportional to  $\delta(M^2 - M'^2)$ , and (2) becomes

$$\sigma^{\gamma^* p}(s, Q^2) = \sum_q \int \frac{dM^2}{(M^2 + Q^2)^2} \rho(s, M^2) \sigma_{q\bar{q}+p}(s, M^2), \quad (3)$$

where the spectral function  $\rho(s, M^2)$  is the density of  $q\bar{q}$  states, which may be expressed in terms of the  $\gamma^* \rightarrow q\bar{q}$  matrix element [17]. Using that  $M^2 = (k_\perp^2 + m_q^2)/[z(1-z)]$ , where  $k_\perp$  and  $z$  are the transverse and longitudinal momentum components of the quark with mass  $m_q$ , we can express the integral over the mass  $M$  of the  $q\bar{q}$  in terms of a two-dimensional integral over  $z$  and  $k_\perp$ . Instead of  $k_\perp$ , it is useful to work with the transverse coordinate  $r_\perp$  (impact parameter representation), which is the variable Fourier conjugate to  $k_\perp$ , resulting [15],

$$\sigma_{L,T}^{\gamma^* p}(x, Q^2) = \int dz d^2 r_\perp |\Psi_{L,T}(z, r_\perp, Q^2)|^2 \sigma_{dip}(x, r_\perp),$$

where  $\sigma_{dip} = \sigma_{q\bar{q}+p}$  and  $x \simeq Q^2/W_{\gamma p}^2$  ( $s = W_{\gamma p}^2$ ) is equivalent to the Bjorken variable. In general, the photon wave functions  $\Psi_{L,T}$  are determined from light cone perturbation theory [15].

The dipole hadron cross section  $\sigma_{dip}$  contains all information about the target and the strong interaction physics. At leading order,  $\sigma_{q\bar{q}} = \frac{C_F}{C_A} (3\alpha_s(\frac{4}{r_\perp^2})/4) \pi^2 r_\perp^2 x g(x, \frac{4}{r_\perp^2})$ , where  $x g(x, \frac{4}{r_\perp^2})$  is the nucleon gluon distribution. In the linear regime, where the high densities effects can be disregarded, the small  $x$  behavior of the gluon distribution is given by the solutions of the DGLAP [1] and/or BFKL [18] evolution equations. The common feature of these equations is the steep increase of  $x g$  as  $x$  decreases. This steep increase cannot persist down to arbitrarily low values of  $x$  since it violates a fundamental principle of quantum theory, *i.e.* the unitarity. The large values of the gluon distribution in this regime (large occupation number of the soft gluon modes) suggests the use of semi-classical methods, which allow to describe the small- $x$  gluons inside a fast moving nucleus by a classical color field [19]. This color field is driven by a classical Yang-Mills equation whose source term is provided by faster partons. When the energy further increases, the structure of the classical field equations does not

change, but only the correlations of the color source. This change can be computed in perturbation theory, and expressed as a functional renormalization group equation for the weight function, in which the 'fast' partons are integrated out in steps of rapidity and in the background of the classical field generated at the previous step [5]. This approach enables one to calculate cross sections in a high gluon density environment. Recently, this approach has been applied for  $eA$  [20, 21],  $pA$  [21, 22, 23] and  $AA$  processes [24]. Basically, we have that the corrections associated to the high parton density when estimated in the color glass condensate formalism [5], implies that  $\sigma_{dip}$  can be written as

$$\sigma_{dip}(x, r_\perp) = 2 \int d^2 b_\perp [1 - S(x, r_\perp, b_\perp)], \quad (4)$$

where  $S$  is the S-matrix element which encodes all the information about the hadronic scattering, and thus about the non-linear and quantum effects in the hadron wave function. (3)

## 2.1 Geometric Scaling

The function  $S$  can be obtained by solving an appropriate evolution equation in the rapidity  $y \equiv \ln(1/x)$  [9, 5]. The main properties of  $S$  are: (a) for the interaction of a small dipole ( $r_\perp \ll 1/Q_s$ ),  $S(r_\perp) \approx 1$ , which characterizes that this system is weakly interacting; (b) for a large dipole ( $r_\perp \gg 1/Q_s$ ), the system is strongly absorbed which implies  $S(r_\perp) \ll 1$ . This property is associated to the large density of saturated gluons in the hadron wave function. The phenomenological saturation model proposed in Ref. [6] encodes the main properties of the saturation approaches. In this model

$$\frac{\sigma_{dip}(x, r_\perp)}{\sigma_0} = 1 - S(x, r_\perp); \quad S = \exp \left[ -\frac{Q_s^2(x) r_\perp^2}{4} \right], \quad (5)$$

with  $\sigma_{dip}/\sigma_0$  the scattering amplitude, averaged over all impact parameters  $b_\perp$ , and  $Q_s^2 \simeq \Lambda^2 e^{\lambda \ln(x_0/x)}$ . The parameters of the model were constrained from the HERA small  $x$  data, coming out typical values of order 1-2 GeV<sup>2</sup> for the momentum scale. We have that when  $Q_s^2(x) r_\perp^2 \ll 1$ , the model reduces to color transparency, whereas as one approaches the region  $Q_s^2(x) r_\perp^2 \approx 1$ , the exponential takes care of resumming many gluon exchanges, in a Glauber-inspired way. Intuitively, this is what happens when the proton starts to look dark. The saturation model depends upon the variables  $x$  and  $r_\perp$  only through the dimensionless quantity  $Q_s r_\perp$ . Consequently, the saturation model predicts the geometric scaling of the total cross section. As demonstrated in Ref. [25], the HERA data on the proton structure function  $F_2$  are consistent with scaling at  $x \leq 0.01$  and  $Q^2 \leq 400$  GeV<sup>2</sup>. Similar behavior has been observed in exclusive [26] and electron-nuclei processes [27].

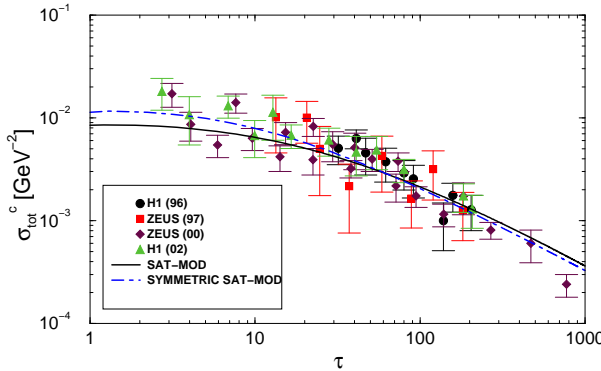


Figure 2. Experimental data on inclusive charm production plotted versus the scaling variable  $\tau = Q^2/Q_s^2$  [28].

Recently, we have demonstrated [28] that the inclusive charm production also exhibits geometric scaling in a large region of photon virtualities, as verified in Fig. 2. In the HERA kinematic domain the saturation momentum  $Q_s^2(x)$  stays below the hard scale  $\mu_c^2 = 4m_c^2$ , implying that charm production probes mostly the color transparency regime and saturation corrections are not very important. The curves are our predictions for the geometric scaling considering two different saturation models, which relies on quite simple assumptions about the dipole-proton interaction. The presence of the geometric scaling in a kinematical region above the saturation scale agrees with recent studies. In particular, in Ref. [29] the authors have demonstrated that the geometric scaling predicted at low momenta  $Q^2 \leq Q_s^2(x)$  is preserved by the BFKL evolution (at both fixed and running coupling constant) up to relatively large virtualities, within the kinematical window  $1 \leq \ln \tau \ll \ln(Q_s^2/\Lambda_{\text{QCD}}^2)$ . On the other hand, in Ref. [30], the impact of the QCD DGLAP evolution on the geometric scaling has been studied. In this case, the DGLAP evolution equation is solved imposing as initial conditions along the critical line  $Q^2 = Q_s^2(x)$  satisfying scaling, showing that it is approximately preserved at very small  $x$ . The residual scaling violation is factored out, although the determination of a window for the scaling above  $Q_s$  is not provided. It is important to emphasize that our results for the nuclear heavy quark photoproduction indicate that the geometric scaling should also be present in the nuclear case [31].

## 2.2 The nuclear structure function

In recent years several experiments have been dedicated to high precision measurements of deep inelastic lepton scattering (DIS) off nuclei. Experiments at CERN and Fermilab focus especially on the region of small values of  $x$ . The data [32], taken over a wide kinematic range, have shown that the proton and neutron structure functions are modified by a nuclear environment. The modifications depends on the parton momentum fraction: for momentum fractions  $x < 0.1$  and  $0.3 < x < 0.7$ , a depletion is observed in the nuclear structure functions. The low  $x$  (shadowing region) and the larger  $x$  (EMC region) are bridged by an enhancement known as antishadowing for  $0.1 < x < 0.3$ . We refer to the entire

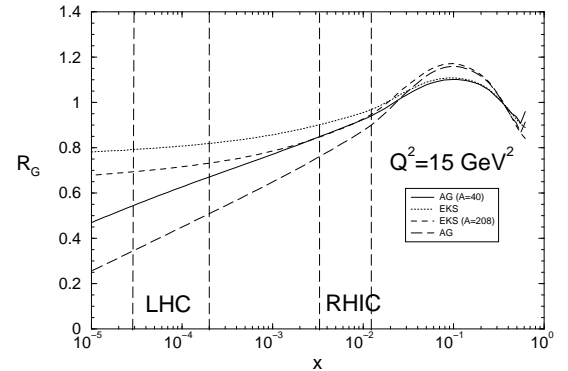


Figure 3. Comparison between the ratio  $R_G$  with and without the high density effects for  $A=40$  (Ca) and  $A=208$  (Pb). The RHIC and LHC kinematic regions are also shown [39].

phenomena as the nuclear shadowing effect. The theoretical understanding of  $F_2^A$  in the full kinematic region has progressed in recent years, with several models which describe the data quite successfully [33]. On the other hand, the saturation effects should also modify the behavior of the nuclear structure function  $F_2^A(x, Q^2)$  [34, 35] and its logarithmic slope [8] at small  $x$ .

One approach to estimate the high density effects in nuclear processes is the Glauber multiple scattering theory [36], which was derived in QCD [37]. In this framework the nuclear collision is analyzed as a succession of independent collisions of the probe with individual nucleons within the nucleus, which implies that [10]

$$S = \exp \left[ -\frac{Q_s^2(x, A)s(b_\perp)r_\perp^2}{4} \right], \quad (6)$$

where  $Q_s^2(x, A)$  is given by Eq. (1) and  $s(b_\perp)$  is the nuclear profile function. In Ref. [35] we have estimated the high density effects in the nuclear structure function and proposed a procedure to obtain a parameterization for the parton distributions which includes the high density and nuclear shadowing effects. In order to illustrate our results, in Fig. 3 we compare our predictions for the  $x$ -dependence of the ratio  $R_G = xg_A(x, Q^2)/xg_N(x, Q^2)$  for  $Q^2 = 15$  GeV $^2$  with the EKS predictions [38], which is derived considering the linear DGLAP dynamics. The results are shown for two typical nuclei of interest in nuclear collisions. Also the corresponding kinematic region which will be explored in the RHIC and LHC colliders are presented. Two important features of the high density effects can be seen in Fig. 3: the magnitude of the effects and the saturation behavior. The suppression of the gluon distribution in respect to the EKS set is 6% for  $A=40$  (Ca) and 11% for  $A=208$  (Pb) in the lower limit of the RHIC kinematic range. When the lower limit of the LHC kinematic range is concerned, the reduction of the gluon distribution is 31% for  $A=40$  and 50% for  $A=208$ . This strong effect also modify the saturation of the ratio predicted in the EKS parameterization at low  $x$ . Basically, in the EKS approach the saturation of the ratio is assumed in the nonperturbative initial condition as a constrain for the behavior of the nuclear parton distributions in

the small  $x$  limit. This behavior is preserved by the DGLAP evolution, since these equations reduce to the DLA limit at low  $x$  in the nucleon and nuclear case, keeping the ratio constant. When the high density effects are considered in the dynamics, a large modification of the gluon distribution is predicted, which is amplified in nuclear processes since the nuclear medium amplifies the effects associated to the high parton density. Therefore, the high density approaches predict larger effects in the nuclear gluon distribution than the nucleon one, independent of the initial parton distributions used. This expectation is present in the behavior of  $R_G^A(AG)$ , which turn to be much smaller than  $R_G^A(EKS)$  in low  $x$  region. The implications of this behavior in the heavy quark production in  $pA$  collisions has been studied in Ref. [39].

### 2.3 The $F_2^A$ slope

Other important observable which can be useful to constrain the boundary region between the linear and nonlinear dynamics is the nuclear structure function slope. As the behavior of this quantity is strongly dependent of the gluon distribution, we expect distinct behaviors at  $Q^2 > Q_s^2$  and  $Q^2 < Q_s^2$  with the transition point dependent of the values of  $x$  and  $A$ . In Ref. [8] we have estimated the behavior of the  $F_2^A$ -slope in the kinematic regions which could be explored in  $eA$  colliders at HERA and RHIC, as well as for some typical values of the number of nucleons  $A$ . Following [6], we have considered that the Bjorken variable  $x$  and the photon virtuality  $Q^2$  are related by the expression  $x = Q^2/W^2$ , where  $W$  is the  $\gamma^*N$  c.m. energy, and calculate the  $x$  and  $Q^2$  dependences for  $W$  and  $A$  fixed. The Fig. 4 shows the logarithmic  $Q^2$  slope of  $F_2^A$  plotted for some typical values of  $W^2$  and  $A = 197$  as a function of  $Q^2$ . The main aspect in the plot is the presence of a distinct maximum for each slope, dependent of the energy. A similar behavior is verified for different number of nucleons. We can see that at fixed  $A$ , if we increase the value of the energy, the maximum value of the slope occur at larger values of  $Q^2$  (and smaller values of  $x$ ) as obtained for the proton structure function slope [6]. The remarkable properties of the collisions with nuclei targets are the large values of  $Q^2$  for the turnover of  $F_2^A$  slope and the large shift of the turnover at large values of  $Q^2$  with the growth of the energy. These behaviors can be understood intuitively. The turnover is associated with the regime in which the partons in the nucleus form a dense system with mutual interactions and recombinations, with a transition between the linear and nonlinear regime at the saturation scale [Eq. (1)]. As the partonic density growth at larger values of the number of nucleons  $A$  and smaller values of  $x$  we have that, at fixed  $A$ , the saturation scale  $Q_s^2$  will increase at small values of  $x$ , since this is directly proportional to the gluon distribution. Moreover, at fixed energy  $W$ , the same density at  $A = 12, 32, 197$  will be obtained at larger values of  $x$  and  $Q^2$ . These properties of the high density effects are verified in the  $F_2^A$  slope. The main result of our analysis was that the saturation should occur already at rather small distances (large  $Q_s^2$ ) well below where soft dynamics is supposed to set in, justifying the use of perturbative QCD to approach a highly dense system.

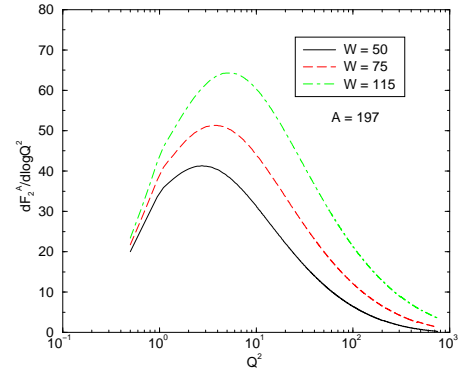


Figure 4. The logarithmic  $Q^2$  slope of  $F_2^A$  as function of the variable  $Q^2$  at different values of  $W$  [8].

### 2.4 The asymptotic regime

The description of the nucleon (nuclear)  $F_2$  and its slope is simplified in the asymptotic regime of very high parton densities. In this case, under the assumption that the interaction is black, we can estimate the total cross section (3) using the following approximations:  $\rho(s, M^2) \propto M^2$  and  $\sigma_{q\bar{q}+p}(s, M^2) = \pi R^2$ . Consequently, we can get  $\sigma^{\gamma^*p}(s, M^2) \propto R^2 \ln[(M_{max}^2 + Q^2)/(M_{min}^2 + Q^2)]$ . Using that  $M_{min}^2 \approx 4m_\pi^2$  whereas  $M_{max}^2 \propto s$ , results that

$$F_2(x, Q^2) = \frac{Q^2}{4\pi\alpha_{em}} \sigma^{\gamma^*p} \propto Q^2 R^2 \ln \frac{1}{x}, \quad (7)$$

which is the black disc limit for the  $F_2$  structure function. This bound, derived from a geometrical analysis, represents the maximum value allowed for the cross sections at high energies (high densities). In Ref. [40] we have analyzed some distinct high energy approaches and demonstrated that this prediction is a common limit. In particular, from the results for the structure function in the asymptotic regime we have verified that this regime is characterized by the identity

$$\frac{dF_2(x, Q^2)}{d\ln Q^2} = F_2(x, Q^2), \quad (8)$$

which is an important signature of the asymptotic regime of high density QCD. This regime should be reached for the case of an interaction with nuclei at smaller parton densities than in a nucleon, since  $Q_s^2(x; A) = A^{1/3} \times Q_s^2(x)$ , where  $Q_s^2(x)$  is the nucleon saturation scale.

## 3 Saturation in Ultraperipheral Heavy Ion Collisions

The studies of saturation effects in nuclear processes show that future electron-nucleus colliders at HERA and RHIC, probably could determine whether parton distributions saturate and constrain the behavior of the nuclear gluon distribution in the full kinematical range. However, until these colliders become reality we need to consider alternative searches

in the current and/or scheduled accelerators which allow us to constrain the QCD dynamics. Recently, we have analyzed the possibility of using ultraperipheral heavy ion collisions as a photonuclear collider (For a review see Ref. [41]). In particular, we have studied the  $J/\Psi$  production [42] and the heavy quark production [43] assuming distinct approaches for the QCD evolution. In this section we present a brief review of the approach and indicate the original references for more details.

In heavy ion collisions the large number of photons coming from one of the colliding nuclei will allow to study photoproduction, with energies  $W_{\gamma N}$  reaching to 950 GeV for the LHC. The photonuclear cross sections are given by the convolution between the photon flux from one of the nuclei and the cross section for the scattering photon-nuclei, with the photon flux  $\frac{dN(\omega)}{d\omega}$  given by the Weizsäcker-Williams method [44, 41]. The final expression for the production of heavy quarks in ultraperipheral heavy ion collisions is given by,

$$\sigma_{AA \rightarrow Q\bar{Q}X} \left( \sqrt{S_{NN}} \right) = \int_{\omega_{min}}^{\infty} d\omega \frac{dN(\omega)}{d\omega} \times \sigma_{\gamma A \rightarrow Q\bar{Q}X} \left( W_{\gamma A}^2 = 2\omega \sqrt{S_{NN}} \right) \quad (9)$$

where  $\omega_{min} = M_{Q\bar{Q}}/4\gamma_L m_p$  and  $\sqrt{S_{NN}}$  is the c.m.s energy of the nucleus-nucleus system. The Lorentz factor for LHC is  $\gamma_L = 2930$ , giving the maximum c.m.s.  $\gamma N$  energy  $W_{\gamma A} \approx 950$  GeV. The typical values of  $x$  which will be probed in ultraperipheral heavy ion collisions, are given by  $x = (M_{Q\bar{Q}}/2p)e^{-y}$ , where  $M_{Q\bar{Q}}$  is the invariant mass of the photon-gluon system and  $y$  the center of momentum rapidity. For Pb + Pb collisions at LHC energies the nucleon momentum is equal to  $p = 2750$  GeV; hence  $x = (M_{Q\bar{Q}}/5500\text{ GeV})e^{-y}$ . Therefore, the region of small mass and large rapidities probes directly the high energy (small  $x$ ) behavior of the QCD dynamics present in the  $\gamma A$  cross section. This demonstrates that ultraperipheral heavy ion collisions at LHC represents a very good tool to constrain the high energy regime of the QCD dynamics, as already verified for two-photon processes [45].

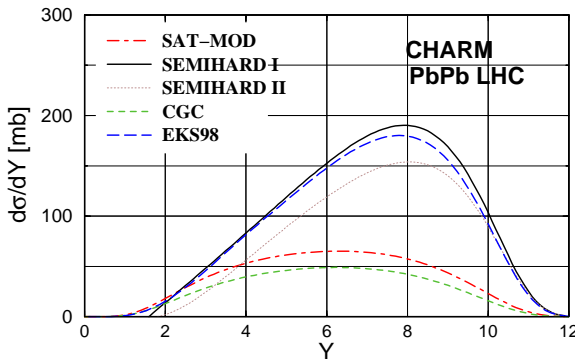


Figure 5. Rapidity distribution for charm production in ultraperipheral heavy ion collisions [43].

In Ref. [43] we have estimated the heavy quark production assuming distinct approaches for the QCD evolution. First, we have considered the usual collinear approach, where the production cross section is driven by the collinear gluon distribution on the nuclei. This one contains a lot of information about nuclear shadowing, EMC, and anti-shadowing effects. Second, the  $k_\perp$ -factorization formalism was introduced, where the relevant quantity is now the nuclear unintegrated gluon distribution. For this purpose, we have analyzed two simple parameterizations for it which are consistent with data description on inclusive and diffractive DIS. Finally, we have taken into account the color glass condensate formalism, where the scattering process is viewed as the interaction of the probe particles with the strong nuclear color field treated in a classical approximation. The main quantity is the correlator of two Wilson lines, which is related to the dipole cross section and at lowest order has no energy dependence. In [43] we have proposed a simple phenomenological parameterization which introduces higher orders corrections to the classical approximation and allow us to produce more realistic estimates for the cross section.

In Fig. 5 is shown the rapidity distribution for the distinct high energy approaches considered. The collinear result is denoted by the long-dashed curves, where we have employed the EKS98 parameterization for the collinear nuclear gluon function. The solid and dotted lines label the semihard ( $k_\perp$ -factorization) results, where one has used that the unintegrated gluon distribution is related to the usual parton distributions by

$$\mathcal{F}_{\text{nuc}}(x, k_\perp^2; A) = \frac{\partial xG_A(x, k_\perp^2)}{\partial \ln k_\perp^2}, \quad (10)$$

where  $xG_A(x, Q^2) = R_g \times xG_N(x, Q^2)$  is the nuclear gluon distribution, with  $R_g$  taken from the EKS parameterization [38]. Two possibilities for the nucleon gluon distribution were considered: (I) GRV94(LO) - solid line - and (II) GRV98(LO) - dotted line. The saturation model results are denoted by the dot-dashed line. In this case we have used the model proposed in Ref. [46], which provides an extension of the  $ep$  saturation model for nuclear processes through Glauber-Gribov formalism. The color glass condensate prediction is denoted by the dashed line. We have that the predictions for the collinear approach and the semihard formalism are similar for both charm and bottom production and give somewhat larger values than the saturation and CGC results. One possible interpretation for the similarity between the predictions of the semihard approach and the collinear one is that the expected enhancement in the  $k_\perp$ -factorization formalism, associated to the resummation of the  $(\alpha_s \ln \frac{\sqrt{s}}{m_Q})^n$  in the coefficient function [4], is not sizeable for inclusive quantities in the kinematic region of the future colliders. Our phenomenological ansatz within the CGC formalism gives similar results as the saturation model, but should be noticed that the physical assumptions in those models are distinct. While the saturation model considers multiple scattering on single nucleons, our expression for the dipole-nucleus cross section in the CGC formalism

assumes scattering on a black area filled by partons coming from many nucleons. It is important to emphasize that the current experimental data for the nuclear structure function can only be described if the first choice is implemented [46]. Our results shown that an experimental analysis of this process can be useful to constrain the QCD dynamics at high energies.

## 4 Saturation in Heavy-Ion Collisions

As we expect that the saturation effects should be manifest in nuclear collisions, the recent results for heavy ion collisions at RHIC have motivated some phenomenological analysis which assume the presence of these effects. In particular, the approach from Ref. [47], which assume saturation of the nuclear wavefunction, describes the experimental data for the multiplicity distributions of produced particles very well. However, the current situation is not unambiguous, since other approaches which do not assume saturation also describe the same set of data. It is important to emphasize that the presence of these effects should modify the behavior of the signatures of the quark-gluon plasma. One of the proposed signatures of the QCD phase transition is the suppression of quarkonium production [48]. The idea of suppression of  $c\bar{c}$  mesons  $J/\psi$ ,  $\psi'$ , etc., is based on the notion that  $c\bar{c}$  are produced mainly via primary hard collisions of energetic gluons during the preequilibrium stage up to shortly after the plasma formation (before the initial temperature drops below the production threshold), and the mesons formed from these pairs may subsequently experience deconfinement when traversing the region of the plasma. In a QGP, the suppression occurs due to the shielding of the  $c\bar{c}$  binding potential by color screening, leading to the breakup of the resonance. The  $c\bar{c}(J/\psi, \psi', \dots)$  and  $b\bar{b}(\Upsilon, \Upsilon', \dots)$  resonances have smaller radii than light-quark hadrons and therefore higher temperatures are needed to dissociate these quarkonium states.

The probability of a thermalized QGP production and the resulting strength of its signatures strongly depends on the initial conditions associated to the distributions of partons in the nuclear wave functions. As discussed above, at very high energies, the growth of parton distributions should saturate. Some years ago, Mueller has proposed idealized initial conditions for a saturated nuclear wave function and shown that the evolution of single particle distributions could be described by a nonlinear Landau equation [49]. One of the main conclusions of that study was that the equilibration time and the initial temperature of the plasma have a strong functional dependence on the initial gluon saturation scale  $Q_s$ . As a direct consequence, the possible signatures of this saturated gluon plasma should be  $Q_s$ -dependent if the saturation scenario is valid for RHIC and LHC. We denote saturated gluon plasma, the plasma formed from the collision of two nuclei with saturated nuclear wave functions. In Ref. [50] we have analyzed the quarkonium suppression as a probe of a saturated gluon plasma. In particular, we have estimated the quarkonium suppression and its dependence in the saturation scale at LHC energies. Below we present a brief review of the main results of that analyses.

Lets start from a brief review of the quarkonium suppression in heavy-ion collisions. The heavy quark pair leading to the quarkonia are produced in such collisions on a very short time-scale  $\sim 1/2m_Q$ , where  $m_Q$  is the mass of the heavy quark. The pair develops into the physical resonance over a formation time  $\tau_f$ . For a confined surrounding, the bound states of  $c\bar{c}$  and  $b\bar{b}$  interacting via two forces: a linear confining potential and a color-Coulomb interaction. In the plasma phase, the linear potential is absent due to the high temperature leading to deconfinement and the color charge is Debye screened by a cloud of surrounding quark-antiquarks pairs which weaken the binding force between the  $Q\bar{Q}$  pair, thus reducing the color charge seen by the other (anti)quark. Basically, above the critical temperature  $T_c$ , we have

$$V(r) = -\frac{\alpha}{r} + \sigma r \Rightarrow V(r) = -\frac{\alpha}{r} \exp(-\mu_D r)$$

where  $\alpha$  and  $\sigma$  (the string tension) are phenomenological parameters and  $\mu_D$  is the Debye mass. For values of the screening mass above a certain critical value  $\mu_i^{diss}$  ( $i = J/\psi, \psi', \chi_c, \Upsilon, \Upsilon', \chi_b$ ), the screening become strong enough for binding to be impossible and the resonance no longer forms in the plasma. As a result, the  $Q$  and  $\bar{Q}$  drift away from each other, after leaving the interacting system to form a charm and bottom mesons, which subsequently decays into leptons to be detected. Therefore, a procedure to determine if quarkonium suppression is expected is the analysis of the screening mass. Basically, if we known the evolution of the screening mass during the collision process we can estimate what quarkonia will be effectively suppressed. At screening mass values greater than  $\mu_i^{diss}$  for values of time above (or equal) to the formation time of the bound state ( $\tau_F$ ), the bound state does not be formed. Therefore, we can analyze the quarkonium suppression considering the dynamical evolution of the screening mass. In Ref. [50] we have obtained an expression for the screening mass in terms of the saturation scale, which is

$$\mu^2 = \left(\frac{c\alpha_s N_c}{\pi}\right)^{\frac{2}{3}} \frac{Q_s^2}{(Q_s t)^{2/3}} . \quad (11)$$

We have concentrated our analysis in the  $\Upsilon$  suppression at LHC energies, since at current energies, the situation of  $J/\psi$  suppression is rather ambiguous because the bound state can also break up through interactions with nucleons and comoving hadrons, i.e., QGP production has not been proved to be the unique explanation of the observed suppression even though an increased density of secondary production is needed (See more details in that follows).

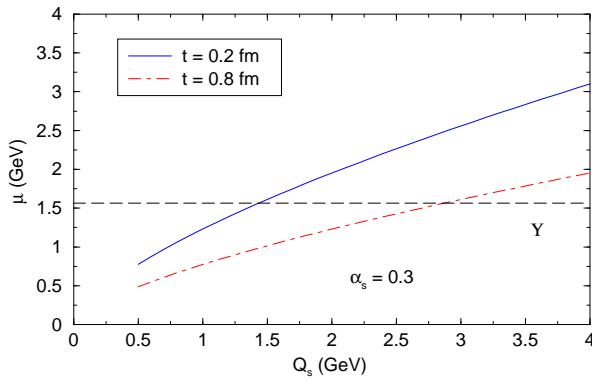


Figure 6. The dependence of the screening mass in the saturation scale for two instants in the saturated plasma evolution. The long dashed curve characterizes the dissociation screening mass for the meson  $\Upsilon$  [50].

In Fig. 6 we present the dependence of the dynamical screening mass in the saturation scale for a typical value of the coupling constant. We verify that the dissociation of the  $\Upsilon$  must occur only if the saturated gluon plasma is characterized by large values of the momentum saturation scale. In other words, the presence of  $\Upsilon$  suppression indicates that if a saturation scenario is valid, the initial nuclear wave function are characterized for a bulk momentum scale  $Q_s \geq 1.5$  GeV. Therefore, the  $\Upsilon$  suppression may be an indirect probe of the nuclear wave functions, and consequently, from the Color Glass Condensate, allowing to constrain the initial gluon saturation scale.

Other possible approach to estimate the high density effects in nuclear  $J/\Psi$  production was recently considered in Ref. [51]. There we have assumed that the collinear factorization approach is still valid for LHC energies and included the high density effects as estimated in the parameterization proposed in Ref. [35]. In particular, we have considered that the  $J/\Psi$  production can be described by the color evaporation model (CEM) [52]. Consequently,

$$\sigma_{AB \rightarrow J/\psi X} = K \sum_{a,b} \int dq^2 \left( \frac{\hat{\sigma}_{ab \rightarrow c\bar{c}}(Q^2)}{Q^2} \right) \int dx_F \phi_{a/A}(x_a) \phi_{b/B}(x_b) \frac{x_a x_b}{x_a + x_b} F_{c\bar{c} \rightarrow J/\psi}(q^2), \quad (12)$$

where  $\sum_{a,b}$  runs over all parton flavors,  $Q^2 = q^2 + 4m_c^2$ ,  $\phi_{a/A}(x_a)$  is the distribution function of parton  $a$  in hadron  $A$ ,  $x_F = x_a - x_b$  and  $x_a x_b = Q^2/s \equiv \tau$ . The  $K$ -factor takes into account the next-to-leading order corrections to the cross section. Moreover, the factor  $F_{c\bar{c} \rightarrow J/\psi}(q^2)$  describes the transition probability for the  $c\bar{c}$  state of the relative square momentum  $q^2$  to evolve into a physical  $J/\psi$  meson. The final state interactions of the produced  $c\bar{c}$  pairs were estimated using the model proposed in Ref. [53], which implies

$$F_{c\bar{c} \rightarrow J/\psi}(\bar{q}^2) = F_{c\bar{c} \rightarrow J/\psi}(q^2 + \varepsilon^2 L), \quad (13)$$

where  $L$  is the effective length of the nuclear medium in the  $AB$  collisions and  $\varepsilon^2$  is the energy gained by the produced  $c\bar{c}$  pair per unit length. The above behavior implies that for a

large enough  $L$ , such that for  $\bar{q}^2 > 4m_D^2 - 4m_c^2$ , the transition probability essentially vanishes due to the existence of the open charm threshold. In Fig. 7 we show our result for the medium length dependence of the  $J/\Psi$  cross section and LHC energy using the distinct parameterizations as input in our calculations. We have assumed  $\varepsilon^2 = 0.250$  GeV $^2$ /fm, which has been constrained using the NA50 data. It is important to emphasize that our model describes very well this set of data. We can see by the comparison between the EKS and AG curve, which includes high density effects, that for LHC energies these effects present in the initial state cannot be disregarded. Moreover, the inclusion of these effects implies an additional  $J/\Psi$  suppression. Therefore, for LHC energies, we predict that these effects strongly reduces the  $J/\Psi$  production rate. This effect is associated to the dominance of the small- $x$  behavior of the nuclear parton distributions at high energies. These results demonstrate that the high density effects will significantly contribute in the nuclear  $J/\Psi$  production, which implies that a careful disentangling of initial and final state effects is required before the clear identification of a new state of matter.

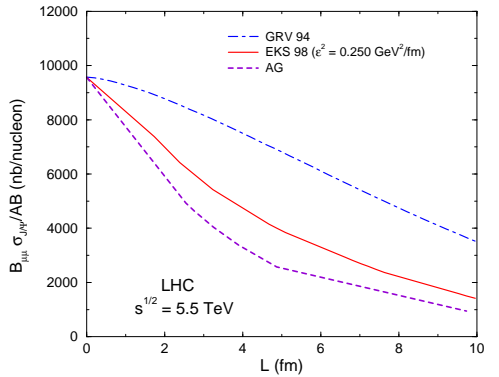


Figure 7. Total  $J/\Psi$  cross sections with the branching ratios to  $\mu^+ \mu^-$  in  $AA$  collisions, as a function of the effective nuclear lenght  $L(A, B)$  [51].

## 5 Summary

The perturbative QCD has furnished a remarkably successful framework to interpret a wide range of high energy lepton-lepton, lepton-hadron and hadron-hadron processes. Through global analysis of these processes, detailed information on the parton structure of hadrons, especially the nucleon, has been obtained. The existing global analysis have been performed using the standard DGLAP evolution equations. However, in the small  $x$  region the DGLAP evolution equations are expected to breakdown, since new dynamical effects associated to the high parton density must occur in this kinematical region.

Research in the field of QCD at high parton density deals both with fundamental theoretical issues, such as unitarity of strong interactions at high energies, and with the challenge of describing experimental data coming, at present, from HERA and RHIC and expected exciting physics of forthcoming experiments at LHC. Over the past few years much

theoretical effort has been devoted towards the understanding of the growth of the total scattering cross sections with energy. These studies are mainly motivated by the violation of the unitarity (or Froissart) bound by the solutions of the linear perturbative DGLAP and BFKL evolution equations. Since these evolution equations predict that the cross section rises obeying a power law of the energy, violating the Froissart bound, unitarity corrections are expected to stop its further growth.

In this paper we have presented a brief review of the basic concepts present in the high density approaches and discussed some aspects of the rapidly developing field of QCD at high parton density in  $e\mu$ ,  $eA$  and  $AA$  collisions. The successful description of all inclusive and diffractive deep inelastic data at the collider HERA, as well as some recent results from RHIC, by saturation models suggests that these effects might become important in the energy regime probed by current colliders. In particular, the remarkable property of geometric scaling verified in the data indicate that the experiments are in a kinematical region which probe QCD in the non-linear regime of high parton density. Moreover, we have verified that deeply inelastic scattering of electrons off nuclei at high energies can determine whether parton distributions saturate. The analysis of the nuclear structure function slope at  $eA$  HERA and/or RHIC energies will allow to establish the presence of a high density system and the behavior of the saturation scale. These results show that the transition between the linear and nonlinear regimes in  $eA$  processes at high energies will occur in a perturbative regime, justifying perturbative QCD approaches. Our recent studies shown that an alternative for  $eA$  colliders is the study of saturation effects in ultraperipheral heavy ion collisions. Furthermore, our results demonstrate that the high density effects are very important mainly at the LHC kinematic region, where strong modifications in the Drell-Yan and quarkonium production are expected. As the small  $x$  behavior of the parton densities strongly determines the initial conditions of the minijet system in nucleus-nucleus collisions, we have that the high density effects cannot be disregarded in the calculations of the observables and signatures of a Quark-Gluon Plasma.

### Acknowledgments

It is a pleasure to acknowledge fruitful discussions and collaborations with my friends A. Ayala Filho, C. A. Berthulani, M. A. Betemps, M. B. Gay Ducati, M. V. T. Machado, L. F. Mackedanz, C. B. Mariotto and W. Sauter. This work was partially financed by the Brazilian funding agencies CNPq and FAPERGS.

### References

- [1] V.N. Gribov and L.N. Lipatov, Sov. J. Nucl. Phys. **15**, 438 (1972); G. Altarelli and G. Parisi, Nucl. Phys. **B126**, 298 (1977); Yu.L. Dokshitzer, Sov. Phys. JETP **46**, 641 (1977).
- [2] A. H. Mueller. Phys. Lett. B **396**, 251 (1997).
- [3] J.C. Collins, D.E. Soper, G. Sterman, Factorization of hard processes in QCD. In: MUELLER, A. H. (Ed.) *Perturbative quantum chromodynamics*. Singapore: World Scientific, 1989.
- [4] S. Catani, M. Ciafaloni, F. Hautmann, Nucl. Phys. **B366**, 135 (1991); J. Collins, R. Ellis, Nucl. Phys. **B360**, 3 (1991); L. Gribov, E. Levin, and M. Ryskin, Phys. Rep. **100**, 1 (1983); E.M. Levin, M.G. Ryskin, YM. Shabelski, and A.G. Shuvaev, Sov. J. Nucl. Phys. **53**, 657 (1991).
- [5] E. Iancu, A. Leonidov, L. McLerran, Nucl. Phys. A **692**, 583 (2001); E. Ferreiro, E. Iancu, A. Leonidov, and L. McLerran, Nucl. Phys. A **703**, 489 (2002); J. Jalilian-Marian, A. Kovner, L. McLerran, and H. Weigert, Phys. Rev. D **55**, 5414 (1997); J. Jalilian-Marian, A. Kovner, and H. Weigert, Phys. Rev. D **59**, 014014 (1999), *ibid.* **59**, 014015 (1999), *ibid.* **59** 034007 (1999); A. Kovner, J. Guilherme Milhano, and H. Weigert, Phys. Rev. D **62**, 114005 (2000); H. Weigert, Nucl. Phys. A **703**, 823 (2002).
- [6] K. Golec-Biernat and M. Wüsthoff, Phys. Rev. D **59**, 014017 (1999), *ibid.* **D60** 114023 (1999).
- [7] M. Gyulassy, L. McLerran, Phys. Rev. C **56**, 2219 (1997).
- [8] V. P. Gonçalves, Phys. Lett. B **495**, 303 (2000); M. B. Gay Ducati and V. P. Goncalves, Phys. Lett. B **466**, 375 (1999).
- [9] Ia. Balitsky, Nucl. Phys. B **463**, 99 (1996); Yu. Kovchegov, Phys. Rev. D **60**, 034008 (1999).
- [10] A. L. Ayala, M. B. Gay Ducati, and E. M. Levin, Nucl. Phys. B **493**, 305 (1997).
- [11] L. V. Gribov, E. M. Levin, and M. G. Ryskin, Phys. Rept. **100**, 1 (1983).
- [12] M. B. Gay Ducati, Braz. J. Phys. **31**, 115 (2001).
- [13] E. Iancu, A. Leonidov, and L. McLerran, arXiv:hep-ph/0202270.
- [14] E. Iancu and R. Venugopalan, arXiv:hep-ph/0303204.
- [15] V. Barone and E. Predazzi, *High-Energy Particle Diffraction*, Springer-Verlag, Berlin Heidelberg, (2002).
- [16] V. N. Gribov. Sov. Phys. JETP **29**, 483 (1969).
- [17] A. Rostovtsev, M. G. Ryskin, and R. Engel. Phys. Rev. D **59**, 014021 (1999).
- [18] L. N. Lipatov, Sov. J. Nucl. Phys. **23**, 338 (1976); E. A. Kuraev, L. N. Lipatov, and V. S. Fadin, JETP **45**, 1999 (1977); I. I. Balitskii, L. N. Lipatov, Sov. J. Nucl. Phys. **28**, 822 (1978).
- [19] L. McLerran and R. Venugopalan, Phys. Rev. D **49**, 2233 (1994), *ibid.* **49**, 3352 (1994), *ibid.* **50**, 2225 (1994).
- [20] L. McLerran and R. Venugopalan, Phys. Rev. D **59**, 094002 (1999); R. Venugopalan, Acta Phys. Polon. B **30**, 3731 (1999).
- [21] F. Gelis and J. Jalilian-Marian, Phys. Rev. D **66**, 014021 (2002); Phys. Rev. D **66**, 094014 (2002); Phys. Rev. D **67**, 074019 (2003).
- [22] A. Dumitru and L. McLerran, Nucl. Phys. A **700**, 492 (2002).
- [23] A. Dumitru and J. Jalilian-Marian, Phys. Lett. B **547**, 15 (2002); Phys. Rev. Lett. **89**, 022301 (2002).
- [24] A. Krasnitz and R. Venugopalan, Nucl. Phys. B **557**, 237 (1999); Phys. Rev. Lett. **84**, 4309 (2000); Phys. Rev. Lett. **86**, 1717 (2001); A. Krasnitz, Y. Nara and R. Venugopalan, Phys. Rev. Lett. **87**, 192302 (2001); Nucl. Phys. A **717**, 268 (2003); arXiv:hep-ph/0305112.

- [25] A. M. Staśto, K. Golec-Biernat and J. Kwieciński, Phys. Rev. Lett. **86**, 596 (2001).
- [26] S. Munier, S. Wallon, Eur. Phys. J. C **30**, 359 (2003).
- [27] A. Freund, K. Rummukainen, H. Weigert, and A. Schafer, Phys. Rev. Lett. **90**, 222002 (2003).
- [28] V. P. Gonçalves and M. V. T. Machado, Phys. Rev. Lett. **91**, 202002 (2003).
- [29] E. Iancu, K. Itakura, and L. McLerran, Nucl. Phys A**708**, 327 (2002).
- [30] J. Kwiecinski and A. M. Stasto, Phys. Rev. D **66**, 014013 (2002).
- [31] V. P. Gonçalves and M. V. Machado, Eur. Phys. J. C **30**, 387 (2003).
- [32] M. Arneodo *et al.*, Nucl. Phys. B **483**, 3 (1997); Nucl. Phys. B **441**, 12 (1995); M. R. Adams *et al.*, Z. Phys. C **67**, 403 (1995).
- [33] See, *e.g.*, M. Arneodo, Phys. Rep. **240**, 301 (1994); G. Piller and W. Weise, Phys. Rep. **330**, 1 (2000).
- [34] M. B. Gay Ducati, V. P. Gonçalves, Phys. Rev. C **60**, 058201 (1999).
- [35] A. L. Ayala Filho and V. P. Gonçalves, Eur. Phys. J. C **20**, 343 (2001).
- [36] R. J. Glauber, Phys. Rev. **100**, 242 (1955); R. C. Arnold, Phys. Rev. **153**, 1523 (1967); T. T. Chou and C. N. Yang, Phys. Rev. **170**, 1591 (1968).
- [37] A. H. Mueller, Nucl. Phys. B **335**, 115 (1990).
- [38] K. J. Eskola, V. J. Kolhinen and C. A. Salgado, Eur. Phys. J. C **9**, 61 (1999).
- [39] A. L. Ayala Filho and V. P. Gonçalves, Phys. Lett. B **534**, 76 (2002).
- [40] M. B. Gay Ducati and V. P. Goncalves, Phys. Lett. B **502**, 92 (2001).
- [41] G. Baur, K. Hencken, D. Trautmann, S. Sadovsky, and Y. Kharlov, Phys. Rept. **364**, 359 (2002).
- [42] V. P. Gonçalves and C. A. Bertulani, Phys. Rev. C **65**, 054905 (2002).
- [43] V. P. Gonçalves and M. V. Machado, Eur. Phys. J. C **31**, 371 (2003).
- [44] C. A. Bertulani and G. Baur, Phys. Rept. **163**, 299 (1988).
- [45] V. P. Gonçalves and M. V. Machado, Eur. Phys. J. C **28**, 71 (2003); Eur. Phys. J. C **29**, 37 (2003); Eur. Phys. J. C **29**, 271 (2003).
- [46] N. Armesto, Eur. Phys. J. C **26**, 35 (2002).
- [47] D. Kharzeev and M. Nardi, Phys. Lett. B **507**, 121 (2001); D. Kharzeev and E. Levin, Phys. Lett. B **523**, 79 (2001); D. Kharzeev, E. Levin, and L. McLerran, Phys. Lett. B **561**, 93 (2003).
- [48] T. Matsui, H. Satz, Phys. Lett. B **178**, 416 (1986).
- [49] A. H. Mueller, Nucl. Phys. B **572**, 227 (2000); Phys. Lett. B **475**, 220 (2000).
- [50] V. P. Goncalves, Phys. Lett. B **518**, 79 (2001).
- [51] M. B. Gay Ducati, V. P. Goncalves, and L. F. Makedanz, Eur. Phys. J. C (in press); arXiv:hep-ph/0306129.
- [52] J. F. Amundson *et al.*, Phys. Lett. B **372**, 127 (1996); M. B. Gay Ducati, C. B. Mariotto, Phys. Lett. B **464**, 286 (1999); M.B. Gay Ducati, G. Ingelman, and C.B. Mariotto, Eur. Phys. J. C **23**, 527 (2002); M. B. Gay Ducati, V. P. Gonçalves, and C. B. Mariotto, Phys. Rev. D **65**, 037503 (2002).
- [53] J. Qiu, J. P. Vary, X. Zhang, Phys. Rev. Lett. **88**, 232301 (2002)